Tumor Suppression by p53 in the Absence of Atm

S. Lawrence Bailey, Kay E. Gurley, Kyung Hoon-Kim, Karen S. Kelly-Spratt, and Christopher J. Kemp

Fred Hutchinson Cancer Research Center, Seattle, Washington

Abstract

Oncogenes can induce p53 through a signaling pathway involving p19/Arf. It was recently proposed that oncogenes can also induce DNA damage, and this can induce p53 through the Atm DNA damage pathway. To assess the relative roles of Atm, Arf, and p53 in the suppression of Ras-driven tumors, we examined susceptibility to skin carcinogenesis in 7,12-dimethylbenz (*a*)anthracene/12-*O*-tetradecanoylphorbol-13-acetate (TPA)–treated Atm- and p53-deficient mice and compared these results to previous studies on Arf-deficient mice. Mice with epidermal-specific deletion of p53 showed increased papilloma number and progression to malignant invasive carcinomas compared with wild-type littermates. In contrast, Atm-deficient mice showed no increase in papilloma number, growth, or malignant progression. γ-H2AX and p53 levels were increased in both $Atm^{+/+}$ and $Atm^{-/-}$ papillomas, whereas $Arf^{-/-}$ papillomas showed much lower p53 expression. Thus, although there is evidence of DNA damage, signaling through Arf seems to regulate p53 in these Ras-driven tumors. In spontaneous and radiation-induced lymphoma models, tumor latency was accelerated in $Atm^{-/-}p53^{-/-}$ compound mutant mice compared with the single mutant $Atm^{-/-}$ or $p53^{-/-}$ mice, indicating cooperation between loss of Atm and loss of p53. Although p53-mediated apoptosis was impaired in irradiated $Atm^{-/-}$ lymphocytes, p53 loss was still selected for during lymphomagenesis in $Atm^{-/-}$ mice. In conclusion, in these models of oncogene- or DNA damage–induced tumors, p53 retains tumor suppressor activity in the absence of Atm.
(Mol Cancer Res 2008;6(7):1185–92)

Introduction

Carcinogenesis is an evolutionary process driven by mutation and selection (1). To intervene in cancer development, it is important to understand the selective pressures that drive tumor evolution. The observation that p53 mutations are found at high frequency in most types of human cancers (2) indicates that selection for cells that have disabled p53 is a nearly universal feature of cancer. p53 can be activated by numerous stressors including DNA damage, oncogene activation, abnormal cell adhesion, altered ribonucleotide pools, hypoxia, telomere erosion, and nutrient deprivation (3, 4). Activated p53, in turn, can suppress tumor development through the induction of cell cycle arrest, senescence, or apoptosis (4). Of the many signals that have been reported to phosphorylate and activate p53, it is unclear which of these is physiologically relevant for tumor suppression *in vivo*. This is further complicated by variations between tissues and tumor etiology. DNA damage and activated oncogenes play direct causal roles in cancer induction and p53 activation, and so both are reasonable candidates for generating selective pressure against p53 during tumor progression.

DNA damage is the best studied activator of p53. DNA double-strand breaks, which can be induced by ionizing radiation or other genotoxic agents, trigger a signaling cascade leading to p53-dependent cell cycle arrest or apoptosis. The protein kinase ATM, which is mutated in the inherited syndrome ataxia telangiectasia, is a primary signal transducer for the cellular response to double-strand breaks (5). DNA double-strand breaks activate ATM, which can directly phosphorylate p53 on Ser^{15} (6, 7). ATM also phosphorylates Chk2, which in turn phosphorylates p53 on Ser^{20} (8, 9). ATM impairs the activity of negative regulators of p53, including the ubiquitin ligases cop1 and mdm2 (10, 11). Collectively, these alterations lead to the rapid accumulation of p53 and activation of its transcriptional functions, which, in turn, can trigger cellular responses such as cell cycle arrest or apoptosis.

Ataxia telangiectasia patients carry homozygous mutations in *ATM* and have an increased risk of developing lymphoreticular malignancies (12). *Atm* knockout mice are highly susceptible to lymphoid malignancies but have not shown a marked predisposition to tumors in other tissues (13, 14). The basis for this tissue specificity is not known. Westphal et al. (15) reported that loss of Atm and p53 cooperate to suppress spontaneous development of lymphomas. Liao et al. (16) showed that p53-dependent tumor suppression in a mouse brain tumor model driven by truncated SV40 T antigen is unaffected by Atm deficiency. In these mouse models, Atm does not seem to be an essential regulator of the tumor suppressor function of p53. Several recent studies showed that Atm deficiency accelerates Myc- and mutant Apc–driven tumors, suggesting that Atm plays a role in these tumor models (17-19).

Atm-dependent signaling *in vivo* is markedly tissue specific. $Atm^{-/-}$ mice have impaired p53-dependent apoptosis in irradiated lymphoid tissue and the developing central nervous

Received 8/29/07; revised 2/13/08; accepted 3/26/08.
Grant support: NIH research grant R01 CA70414 and National Institute of Environmental Health Sciences research grant U01 ES11045.
The costs of publication of this article were defrayed in part by the payment of page charges. This article must therefore be hereby marked *advertisement* in accordance with 18 U.S.C. Section 1734 solely to indicate this fact.
Note: Current address for K. Hoon-Kim: Trubion Pharmaceuticals, Seattle, WA 98121.
Requests for reprints: Christopher J. Kemp, Fred Hutchinson Cancer Research Center, 1100 Fairview Avenue North, Seattle, WA 90109-1024. Phone: 206-667-4252; Fax: 206-667-5815. E-mail: cjkemp@fhcrc.org

doi:10.1158/1541-7786.MCR-07-2009

Table 1. Conversion Frequency of Carcinomas to Papillomas for Mice That Lived at Least 20 Weeks After DMBA

Genotype	No. of Mice	Total No. of Papillomas	Total No. of Carcinomas	Conversion Frequency (%)	P (vs $ATM^{+/+}$)
$ATM^{-/-}$	7	21	6	5.0	1
$ATM^{+/-}$	33	664	55	8.3	.11
$ATM^{+/+}$	25	503	28	5.6	N/A

system as compared with wild-type (WT) mice (20-22). However, after a slight delay, p53 induction and apoptotic responses are largely intact in epithelial cells within hair follicles and intestinal crypts from irradiated *Atm* null mice (23). This indicates that Atm plays a critical role in DNA damage–triggered apoptosis in lymphoid cells but there are alternative pathways in epithelial tissues that can compensate in the absence of Atm. The presence of redundant DNA-damaging signaling pathways in some tissues such as epithelium may explain the narrow tumor spectrum observed in Atm-deficient mice.

A long-standing question about the model where DNA damage provides selective pressure against p53 is the source of DNA damage in tumors. Several recent studies showed that premalignant human lesions have constitutively active DNA damage signaling, as determined by staining for γ-H2AX, activated ATM, Chk2, and p53 (24, 25). It was further shown that oncogenes such as Ras can induce DNA damage and Atm signaling, which can then trigger p53-mediated senescence and tumor suppression (26, 27). Here we test the role of Atm during tumor evolution by comparing the effects of Atm and p53 loss in epithelial and lymphoid tumor models.

Results

We first tested the role of Atm in suppressing Ras-driven tumors by examining the susceptibility of Atm-deficient mice to 7,12-dimethylbenz(*a*)anthracene (DMBA)/12-*O*-tetradecanoylphorbol-13-acetate (TPA)–induced skin tumors. This protocol involves the topical application of the carcinogen DMBA to the dorsal skin, followed by twice weekly applications of the tumor promoter TPA. This induces benign squamous cell papillomas, a small percentage of which can progress to malignant squamous cell carcinomas after a long latency. Mutation of *Hras* is the initiating event in this tumor model and is detected in ~90% of both papillomas and carcinomas (28). Mutational inactivation of p53 occurs late and is strongly associated with papilloma to carcinoma conversion (29). A causal role for p53 in malignant progression was established using germ-line *p53* knockout mice, which showed a markedly accelerated rate of carcinoma formation (30). That mutations in *Hras* and *p53* occur reproducibly at defined stages in this model facilitates the evaluation of the interaction between Atm and these cancer genes in the context of developing autochthonous tumors.

One hundred percent of DMBA/TPA–treated $Atm^{+/+}$, $Atm^{+/-}$, and $Atm^{-/-}$ mice developed papillomas, which first appeared between 7 and 9 weeks after DMBA treatment. The average number of papillomas per mouse was similar for all genotypes through 25 weeks of observation (Fig. 1B). The growth rate of papillomas, as measured by tumor size, was also similar for all genotypes through 15 weeks but slightly reduced in *Atm*-null mice after 15 weeks (Fig. 1A). Carcinomas first appeared in $Atm^{+/+}$, $Atm^{+/-}$, and $Atm^{-/-}$ mice at 15, 22, and 25 weeks, respectively. The latency to carcinoma formation is shown by Kaplan-Meier plots in Fig. 1C. The median age for carcinoma development was 29, 32, and 27 weeks for $Atm^{+/+}$, $Atm^{+/-}$, and $Atm^{-/-}$ mice, respectively, and these values were not significantly different. However, during the course of this study, many Atm null mice died of lymphomas (Fig. 1D), and some of these died before any reasonable chance of progression to carcinomas. Therefore, we also analyzed the conversion frequency of papillomas to carcinomas for mice that lived at least 20 weeks after DMBA. Table 1 shows that the percentage of papillomas that progressed to carcinomas was 5.6%, 8.3%, and 5.0% in $Atm^{+/+}$, $Atm^{+/-}$, and $Atm^{-/-}$ mice, respectively. These frequencies were not significantly different using two-sided Fisher's exact test. Taken together, these results show that homozygous or hemizygous Atm deficiency did not significantly enhance Hras-driven tumor number, growth rate, or malignant progression.

To compare these results to the effects of p53 loss on skin tumor progression, we repeated the DMBA/TPA protocol on p53-deficient mice. We previously reported accelerated

Table 2. Tumor Spectrum in Atm- (AT) and p53-Deficient Mice

	Spontaneous				Irradiated			
	$AT^{-/-}p53^{-/-}$	$AT^{-/-}p53^{+/-}$	$AT^{-/-}p53^{+/+}$	$AT^{+/+}p53^{-/-}$	$AT^{-/-}p53^{-/-}$	$AT^{-/-}p53^{+/-}$	$AT^{-/-}p53^{+/+}$	$AT^{+/+}p53^{-/-}$
Thymoma/Lymphoma	9	9	12	9	4	11	4	8
Sarcoma	1	0	0	2	0	0	0	1
Testicular Tumor	0	0	0	2	0	0	0	2
Brain Tumor	0	0	0	1	0	0	0	0
Multiple	2	1	0	2	0	0	0	0
Other	1	1	2	1	0	0	1	0
Total	13	11	14	17	4	11	5	11

malignant progression in germ-line p53-deficient mice (30) and here we show similar effects with conditional p53-deficient mice (see Materials and Methods; ref. 31). The average number of papillomas was similar between *Trp53*$^{F2\text{-}10/F2\text{-}10}$; *K14-Cre* (skin-specific p53 deficient) and *Trp53*$^{F2\text{-}10/F2\text{-}10}$ (p53 WT) mice through 15 weeks. However, new tumors continued to appear in p53-deficient mice after this time while plateauing in the WTs (Fig. 1E). Carcinomas first appeared in *Trp53*$^{F2\text{-}10/F2\text{-}10}$; *K14-Cre* mice at 15 weeks, and by 30 weeks, 75% of conditional p53-deficient mice averaged two carcinomas per mouse (Fig. 1F). In contrast, WT littermates did not develop any carcinomas until after 30 weeks. This difference was highly significant (P = 0.001). Thus, skin-specific p53 deletion markedly accelerates malignant skin tumor progression, a result similar to that seen in p53 germ-line nullizygous mice (30, 32). This establishes that the effect of p53 on inhibiting malignant progression is tumor cell autonomous. Both the Atm and p53 skin tumor studies were done using littermate WT controls. This is important because the WT mice from the two studies differed in carcinoma susceptibility, likely due to different genetic backgrounds (see Materials and Methods). Comparison between these two skin tumor studies reveals that p53 has a more significant effect on suppressing Ras-driven tumor progression than does Atm.

We next addressed if DNA damage signaling was prominent in papillomas and if this led to Atm-dependent expression of p53. H2AX is rapidly phosphorylated in response to DNA double-strand breaks (33) and phospho-H2AX (γ-H2AX) is widely used as a marker of DNA damage. However γ-H2AX also increases in M-phase cells without DNA damage (34, 35) and can be readily detected in epithelial cells during the hair cycle phase in untreated mouse skin (36). Staining for γ-H2AX was seen in the occasional cell within the hair follicle of normal skin and in basal and suprabasal cells of the papillomas (Fig. 2A). Although Atm can phosphorylate H2AX after ionizing radiation (37), we observed similar levels of γ-H2AX staining in papillomas from *Atm*$^{+/+}$ and *Atm*$^{-/-}$ mice, indicating that there are kinases that can substitute for Atm to phosphorylate H2AX *in vivo*. Despite γ-H2AX staining, phospho-Chk2, a marker of DNA damage signaling, was low or undetectable in both *Atm*$^{+/+}$ and *Atm*$^{-/-}$

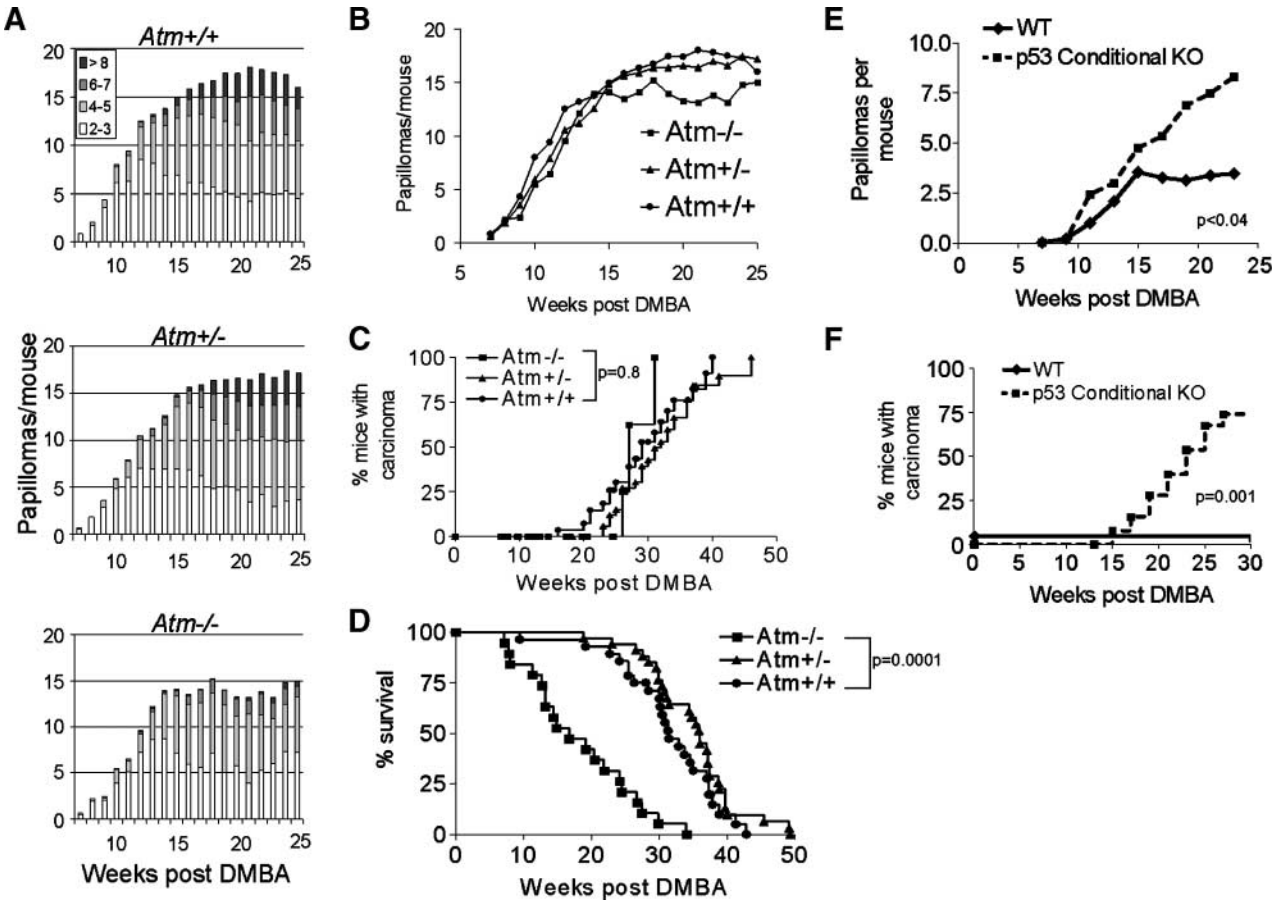

FIGURE 1. Skin tumor development in Atm- and p53-deficient mice. **A.** DMBA/TPA–induced papillomas in Atm-deficient mice. The mean number of papillomas per mouse of the indicated size class is plotted over time after DMBA treatment. **B.** The average number of papillomas of all size classes from mice of the indicated *Atm* genotype is plotted over time after DMBA treatment. **C.** Carcinoma-free survival in DMBA/TPA–treated mice. [P = 0.8, *Atm*$^{-/-}$ versus *Atm*$^{+/+}$; P = 0.2, *Atm*$^{+/-}$ versus *Atm*$^{+/+}$ (log-rank test)]. **D.** Tumor-free survival in DMBA/TPA–treated mice. [P < 0.0001, *Atm*$^{-/-}$ versus *Atm*$^{+/+}$; P = 0.11, *Atm*$^{+/-}$ versus *Atm*$^{+/+}$ (log-rank test)]. **E.** DMBA/TPA–induced papillomas in *Trp53*$^{F2\text{-}10/F2\text{-}10}$ (p53 WT) and *Trp53*$^{F2\text{-}10/F2\text{-}10}$; *K14-Cre* (skin-specific p53 deficient) mice. The number of papillomas in p53-deficient mice at 23 and 25 wk was greater than WTs (P = 0.003 and P = 0.04, respectively, unpaired t test). **F.** Carcinoma-free survival in DMBA/TPA–treated p53 WT and skin-specific p53–deleted mice [p53 conditional knockout (*KO*)]. The difference was highly significant (P = 0.001, log-rank test).

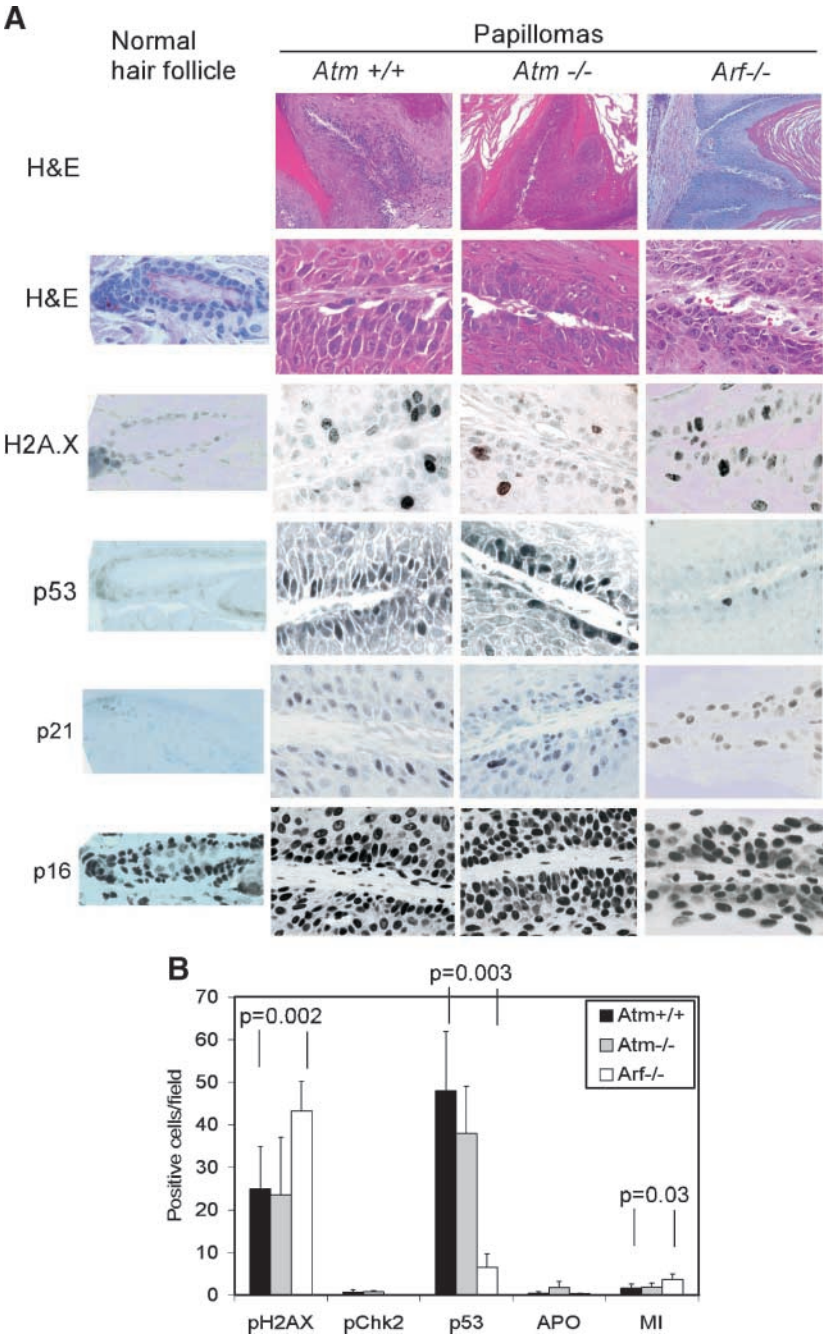

FIGURE 2. DNA damage signaling in Atm-deficient papillomas. **A.** H&E-stained sections and immunostaining for the indicated proteins from papillomas from WT, $Atm^{-/-}$, and $Arf^{-/-}$ mice. Top row was photographed at a final magnification of ×100 and bottom rows at ×600. **B.** Quantification of γ-H2AX, phospho-Chk2 (*pChk2*), p53, apoptosis (*APO*), and mitotic index (*MI*) in $Atm^{+/+}$, $Atm^{-/-}$, and $Arf^{-/-}$ papillomas (n = 5-7 tumors per genotype). Columns, mean number of cells that stained for γ-H2AX, phospho-Chk2, p53, or apoptotic or mitotic figures per 400× field; bars, SD. The P values were determined by the Mann-Whitney test.

papillomas (Fig. 2B). As a positive control, staining for phospho-Chk2 was seen in irradiated intestinal crypts (data not shown). p53 was undetectable in normal skin but prominent in papillomas and primarily localized to keratinocytes within the basal layer (Fig. 2). Equivalent levels and cellular distribution patterns of p53 staining were seen in papillomas from $Atm^{+/+}$ and $Atm^{-/-}$ mice. Expression of the p53-regulated gene *p21* (*Cdkn1a*) and the cyclin-dependent kinase inhibitor p16 (Ink4a) were also seen in both $Atm^{+/+}$ and $Atm^{-/-}$ papillomas. As another measure of p53 functionality, we quantified proliferation and apoptosis. The mitotic index was similar in papillomas from $Atm^{+/+}$ and $Atm^{-/-}$ mice, whereas the apoptotic index, as measured by both active caspase-3 and apoptotic figures, was slightly elevated in $Atm^{-/-}$ papillomas (Fig. 2B). Thus, Atm deficiency did not measurably affect the levels of H2AX, p53, p21, or cell proliferation in benign tumors.

It is useful to compare these results to those seen in p19/Arf null mice. Arf is a tumor suppressor that induces p53 in response to oncogenic activation (38, 39). We previously showed accelerated papilloma to carcinoma progression in Arf-deficient mice using an identical DMBA/TPA protocol (32). In comparison with papillomas from WT and *Atm* null mice, *Arf* null papillomas showed reduced p53 expression and higher

H2AX staining and increased mitotic activity (Fig. 2). This confirms our previous findings that Arf plays a critical role in the induction of p53 during benign tumor growth. Reduced p53 could explain the increased proliferation in these tumors, and this may contribute to increased levels of H2AX. However, the DNA damage p53 pathway is still functional in these tumors because irradiated tumor-bearing $Arf^{-/-}$ mice showed robust p53 induction in papillomas (32). These findings, together with the low levels of phospho-Chk2 in untreated papillomas, show that the levels of DNA damage in untreated tumors may be insufficient to trigger a DNA damage response. Thus, tumor suppression by p53, at least in this model of epithelial cancer, is regulated by Arf, and selection against p53 is driven by oncogenic signaling through Arf.

Compared with epidermal cells, Atm has a more critical role in regulating p53 in lymphoid cells (23), thus we also examined the interaction of Atm and p53 in spontaneous and ionizing radiation–induced lymphoma models. The latency for spontaneous tumor development in $Atm^{-/-}$ mice (median age of death, 116 days) was shorter than for $p53^{-/-}$ mice (median, 141 days; Fig. 3A). Tumor latency was significantly accelerated in $Atm^{-/-}$ $p53^{-/-}$ compound mutant mice (median, 84 days) relative to either single mutant alone, consistent with a previous study (15). Approximately 95% of $Atm^{-/-}$ and $Atm^{-/-}$ $p53^{-/-}$ mice developed CD3-positive T-cell lymphomas, which presented as enlarged thymi, with occasional splenic or lymph node involvement. The tumor spectrum differed slightly in the *p53* nulls; 60% developed thymic lymphoma and 40% developed other tumor types, mainly sarcomas (Table 2). Thus, the reduced tumor latency in $Atm^{-/-}$ $p53^{-/-}$ mice was mainly due to acceleration of T-cell thymic lymphomas.

Ionizing radiation–induced p53 expression and apoptosis are markedly impaired in thymic lymphoid cells from adult Atm null mice (21), indicating that Atm plays a central role in regulating p53 and apoptosis in these cells. We first verified that ionizing radiation–induced apoptosis was impaired in thymocytes from young Atm-deficient mice. Results shown in Fig. 3C show reduced apoptosis in irradiated $Atm^{-/-}$ thymus compared with WT littermates. If this Atm-dependent apoptotic pathway is critical for tumor suppression, a prediction is that germ-line Atm deficiency should effectively neutralize p53 in a radiation-induced tumor model. An additional cohort of mice was treated at 2 days of age with a single dose of 1.4 Gy. Neonatal radiation reduced the latency-to-tumor development in $p53^{-/-}$ mice from a median of 141 days to 100 days (Fig. 3B). However, radiation did not noticeably affect tumor development in $Atm^{-/-}$ mice. The median age to tumor development in irradiated $Atm^{-/-}$ mice was 113 days, compared with 116 days in the nonirradiated cohort. Tumor latency in irradiated $Atm^{-/-}$ $p53^{-/-}$ compound mutants (median, 72 days) was again reduced compared with either single mutant alone. The predominant tumor type in all irradiated genotypes was CD3-positive T-cell lymphomas, with a 95% incidence (Table 2).

We next asked if loss of Atm reduced or eliminated selection against p53 during tumor development by examining loss of heterozygosity of p53 in tumors from $Atm^{-/-}$ $p53^{+/-}$ mice. Fifty percent (4 of 8) of spontaneous thymic lymphomas and 89% (8 of 9) of ionizing radiation–induced lymphomas from $Atm^{-/-}p53^{+/-}$ mice showed loss of the WT *p53* allele (Fig. 4). This is comparable to 57% (4 of 7) loss of p53 in lymphomas from $p53^{+/-}$ mice (Fig. 4) and a range of 43% to 75% p53 loss of heterozygosity reported in previous studies (40-43). Thus, p53 loss occurs in tumors with or without the presence of Atm. Even under conditions where ionizing radiation–induced p53-dependent apoptosis is disabled due to loss of Atm, selection against p53 remains. This indicates that although Atm regulates p53-dependent apoptosis in response to acute DNA damage, other Atm-independent pathways influence the tumor suppressor function of p53, even in a tumor model where DNA damage was the inducing agent. This also implies that apoptosis is not the only mechanism of tumor suppression by p53.

Discussion

Here, we used three mouse models to compare the roles of Atm and p53 in the suppression of oncogene- and DNA

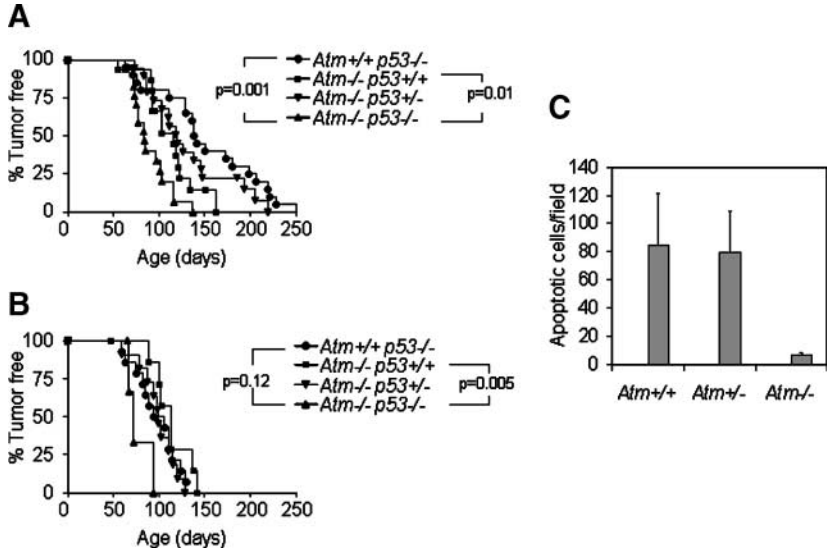

FIGURE 3. Loss of p53 and Atm cooperate during tumorigenesis. **A.** Spontaneous tumor development is accelerated in $Atm^{-/-}$ $p53^{-/-}$ (n = 13) mice relative to $Atm^{-/-}$ (n = 14) or $p53^{-/-}$ (n = 18) mice. **B.** Ionizing radiation–induced tumor development is accelerated in all genotypes except $Atm^{-/-}$ mice. $Atm^{-/-}p53^{-/-}$ mice (n = 4) develop tumors faster than $Atm^{-/-}$ (n = 8) or $p53^{-/-}$ (n = 15) mice. **C.** Ionizing radiation–induced apoptosis in thymus from 3-wk-old mice (4 Gy, 4 h). Columns, mean apoptotic figures per 400× field from three to five mice per genotype; bars, SD.

damage–induced tumor development. We first compared the effect of deletion of Atm and p53 on the progression of chemically induced skin tumors. Approximately 90% of DMBA/TPA–induced papillomas have *Hras* mutations and these tumors showed increased staining for γ-H2AX, p53, and p21 compared with normal skin. However, staining for these markers was not significantly reduced in *Atm* null tumors, indicating that Atm is not required for the activation of this tumor suppressor pathway in this autochthonous tumor model. This is consistent with previous results showing that Atm is dispensable for acute ionizing radiation–induced p53 and apoptosis in epidermal hair follicle cells (23). p53 can be activated by DNA damage in an Atm-independent manner (e.g., through Atr) and these other pathways may compensate for the loss of Atm in regulating p53 in this tissue (44).

Compared with WT and *Atm* null tumors, *Arf* null tumors showed very little p53 expression and increased proliferation. This indicates a central role for Arf in regulating p53 during tumor growth. That acute ionizing radiation was able to induce p53 in *Arf* null tumors (32) shows that exogenous DNA damage can induce p53 in tumors in the absence of Arf. This further implies that the levels of endogenous DNA damage or damage-induced signaling, which is present in untreated tumors, may be insufficient to activate p53.

The affects of Atm, Arf, and p53 on tumor progression were consistent with these signaling results. Deletion of both p53 and Arf, but not Atm, markedly accelerated the progression of benign papillomas to invasive malignant carcinomas. In WT mice, p53 loss is strongly selected for during the progression of papillomas to carcinomas and p53 loss was less frequent in *Arf* null carcinomas. Together these results show that signaling through Arf induces p53, and this provides significant selective pressure against p53.

We also found that the latencies for both spontaneous and radiation-induced lymphomas were accelerated in *Atm p53* compound mutant mice relative to either single mutant alone. This shows that loss of Atm and p53 can cooperate to accelerate tumor formation and that p53 retains tumor suppressor activity in the absence of Atm. Frequent loss of p53 in lymphomas from $Atm^{-/-}$ $p53^{+/-}$ mice indicates that selection against p53 does not require Atm, even in tumors induced by DNA-damaging ionizing radiation. This was surprising because ionizing radiation–induced p53 expression and apoptosis are impaired in *Atm* null lymphocytes. Our results are in general agreement with a classic study by Christophorou et al. (45), which showed that DNA damage–induced apoptosis is irrelevant for tumor suppression by p53. In that study, selection against p53 was instead driven by oncogene-mediated signaling through the p19/Arf tumor suppressor. Liao and Van Dyke (46) also concluded that there were two different mechanisms of tumor suppression by Atm and p53: Lymphoma suppression in *Atm* null mice depended on V(D)J recombination, whereas lymphomas from *p53* null mice arose independently of V(D)J recombination. Atm has recently been implicated in repair of V(D)J breaks during antigen receptor rearrangement, and this function could play a role in lymphoma suppression by minimizing oncogenic translocations (47). Consistent with this idea, translocations involving the antigen receptors are frequently seen in lymphoid tumors from both ataxia telangiectasia patients (48) and $Atm^{-/-}$ mice (20, 21).

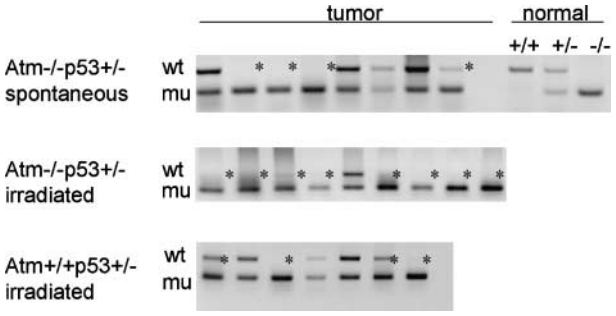

FIGURE 4. p53 loss of heterozygosity is seen in tumors from both $Atm^{+/+}$ and $Atm^{-/-}$ mice. PCR analysis shows loss of the WT allele of *p53* in 4 of 7 spontaneous and 8 of 9 ionizing radiation–induced tumors from $Atm^{-/-}p53^{+/-}$ mice and from 4 of 7 tumors from $p53^{+/-}$ mice. *, loss of heterozygosity of *p53* in tumors. wt, WT p53 allele; mu, mutant *p53* allele.

In summary, the requirement for Atm in regulating p53 in response to DNA damage varies between tissues, and this may at least partially explain the tissue-specific role of Atm in tumor suppression. In the tumor models we examined, loss of Atm did not phenocopy the loss of p53; that is, p53 retained significant tumor suppressor activity in the absence of Atm. This highlights that there are multiple and, in some cases, redundant signals that can activate p53 during tumor suppression. In the case of Ras-driven skin tumors, Arf seems to play a more significant role than Atm in p53 regulation and tumor progression. Identifying the rate-limiting steps in tumor progression in different tumor models and under different tumor etiologies remains an important goal in cancer research. In the broader picture, understanding the nature of the selective pressures that drive tumor evolution is a necessary step to designing effective, mechanistically based interventions.

Materials and Methods

Mice

F_1 NIH/FVB;129 $Trp53^{F2\text{-}10/+}$ mice (31) were crossed to N_1 NIH/C57 *K14-Cre* mice (49) and progeny intercrossed to generate experimental mice with the genotypes $Trp53^{F2\text{-}10/F2\text{-}10}$ (p53 WT) and $Trp53^{F2\text{-}10/F2\text{-}10}$; *K14-Cre* (skin-specific p53 deficient). PCR analysis confirmed that p53 was deleted in epidermis but not in liver, spleen, or thymus. The backs of 8-wk-old p53 functional WT ($n = 22$) and p53 functional null ($n = 29$) mice were shaved and treated with a single application of DMBA (Sigma; 25 μg in 200-μL acetone) followed a week later by twice weekly applications of TPA (Sigma; 200 μL of 10^{-4} mol/L solution in acetone) for 15 wk. The number and size of papillomas on each mouse were recorded every week. Mice were sacrificed if moribund or 1 to 3 wk following detection of carcinomas. All major organs were examined and tumors were frozen for DNA extraction and/or fixed in formalin to be processed and stained with H&E for histologic examination. For the Atm skin tumor study, the *Atm* knockout allele was backcrossed 13 times to the susceptible NIH/Ola strain (Harlan Olac). Experimental mice of all three *Atm* genotypes were then generated from NIH/Ola $Atm^{+/-}$ breeders.

$Atm^{-/-}$ ($n = 18$), $Atm^{+/-}$ ($n = 34$), and $Atm^{+/+}$ ($n = 25$) mice were treated as above. For the spontaneous and radiation-induced tumor models, 129/SvEv $Atm^{+/-}$ (14) and C57BL6 $p53^{+/-}$ mice (50) were intercrossed to generate experimental mice of the requisite combined *Atm* and *p53* genotypes. One cohort was left untreated and an additional cohort was irradiated at 2 d of age (1.4 Gy, using a ^{60}Co irradiator). Experimental mice were sacrificed and necropsied when exhibiting symptoms of tumor burden.

Histologic Analysis

Sections of normal or tumor tissue were removed and either snap frozen or fixed for 4 h in normal buffered formalin and then processed to paraffin. Four-micrometer sections were cut, deparaffinized, and stained for H&E, p53 (Novocastra CM5), p21 (BD PharMingen), p16 (Abcam), cleaved caspase-3 (Asp^{175}) (Cell Signaling Tech 9661), phospho-histone H2AX (Ser^{139}) (Cell Signaling Tech 2577), or phospho-Chk2 (T68) (Abcam). $p19/Arf^{-/-}$ papillomas stained for p53 were from a previous study (32). Staining for all antibodies was done using a three-step streptavidin technique. Sections were rehydrated and treated with high-heat antigen retrieval using a 10 mmol/L citrate buffer (pH 6) and then stained with primary antibody. After staining with the primary antibody, the sections were stained with a biotin-conjugated secondary (Vector labs) followed by StreptABComplex/horseradish peroxidase (DAKO). Slides were developed with 3,3′-diaminobenzidine/NiCl and counterstained with methyl green. Control sections with no primary antibody were run concurrently. Other sections were cut and stained with H&E. Apoptosis, proliferation, and labeling indices were determined by counting the number of stained cells per 400× field in five to seven papillomas per *Atm* genotype. All counts were done with a Nikon Labophot-2 microscope without knowledge of genotype.

p53 Loss of Heterozygosity

Genomic DNA was prepared from tumor tissue or normal kidney with QIAamp DNA Mini Kit (Qiagen). WT and knockout alleles of p53 from tumors from $p53^{+/-}$ mice were amplified in a separate reaction, as described (51), for 30 cycles. PCR products were electrophoresed on a 2% Tris-acetate-EDTA agarose gel. Comparison gradients for p53 were established by combining WT and knockout genomic DNA in quantified ratios, then amplifying as described above.

Disclosure of Potential Conflicts of Interest

No potential conflicts of interest were disclosed.

Acknowledgments

We thank Tony Wynshaw-Boris (Dept. of Pediatrics, University of California, San Diego, La Jolla, CA) for providing *Atm* null mice and members of the Kemp laboratory for helpful discussions.

References

1. Kemp CJ. Multistep skin cancer in mice as a model to study the evolvability of cancer cells. Semin Cancer Biol 2005;15:460–73.

2. Hainaut P, Hollstein M. p53 and human cancer: the first ten thousand mutations. Adv Cancer Res 2000;77:81–137.

3. Giaccia AJ, Kastan MB. The complexity of p53 modulation: emerging patterns from divergent signals. Genes Dev 1998;12:2973–83.

4. Vousden KH, Lu X. Live or let die: the cell's response to p53. Nat Rev Cancer 2002;2:594–604.

5. Shiloh Y. The ATM-mediated DNA-damage response: taking shape. Trends Biochem Sci 2006;31:402–10.

6. Banin S, Moyal L, Shieh S, et al. Enhanced phosphorylation of p53 by ATM in response to DNA damage. Science 1998;281:1674–7.

7. Canman CE, Lim DS, Cimprich KA, et al. Activation of the ATM kinase by ionizing radiation and phosphorylation of p53. Science 1998;281:1677–9.

8. Shieh SY, Ahn J, Tamai K, Taya Y, Prives C. The human homologs of checkpoint kinases Chk1 and Cds1 (Chk2) phosphorylate p53 at multiple DNA damage-inducible sites. Genes Dev 2000;14:289–300.

9. Chehab NH, Malikzay A, Appel M, Halazonetis TD. Chk2/hCds1 functions as a DNA damage checkpoint in G_1 by stabilizing p53. Genes Dev 2000;14:278–88.

10. Maya R, Balass M, Kim ST, et al. ATM-dependent phosphorylation of Mdm2 on serine 395: role in p53 activation by DNA damage. Genes Dev 2001;15:1067–77.

11. Dornan D, Shimizu H, Mah A, et al. ATM engages autodegradation of the E3 ubiquitin ligase COP1 after DNA damage. Science 2006;313:1122–6.

12. Chun HH, Gatti RA. Ataxia-telangiectasia, an evolving phenotype. DNA Repair (Amst) 2004;3:1187–96.

13. Xu Y, Ashley T, Brainerd EE, et al. Targeted disruption of ATM leads to growth retardation, chromosomal fragmentation during meiosis, immune defects, and thymic lymphoma. Genes Dev 1996;10:2411–22.

14. Barlow C, Hirotsune S, Paylor R, et al. Atm-deficient mice: a paradigm of ataxia telangiectasia. Cell 1996;86:159–71.

15. Westphal CH, Rowan S, Schmaltz C, et al. atm and p53 cooperate in apoptosis and suppression of tumorigenesis, but not in resistance to acute radiation toxicity. Nat Genet 1997;16:397–401.

16. Liao MJ, Yin C, Barlow C, Wynshaw-Boris A, Van Dyke T. Atm is dispensable for p53 apoptosis and tumor suppression triggered by cell cycle dysfunction. Mol Cell Biol 1999;19:3095–102.

17. Pusapati RV, Rounbehler RJ, Hong S, et al. ATM promotes apoptosis and suppresses tumorigenesis in response to Myc. Proc Natl Acad Sci U S A 2006;103:1446–51.

18. Maclean KH, Kastan MB, Cleveland JL. Atm deficiency affects both apoptosis and proliferation to augment Myc-induced lymphomagenesis. Mol Cancer Res 2007;5:705–11.

19. Kwong LN, Weiss KR, Haigis KM, Dove WF. Atm is a negative regulator of intestinal neoplasia. Oncogene 2008;27:1013–8.

20. Barlow C, Brown KD, Deng CX, Tagle DA, Wynshaw-Boris A. Atm selectively regulates distinct p53-dependent cell-cycle checkpoint and apoptotic pathways. Nat Genet 1997;17:453–6.

21. Xu Y, Baltimore D. Dual roles of ATM in the cellular response to radiation and in cell growth control. Genes Dev 1996;10:2401–10.

22. Herzog KH, Chong MJ, Kapsetaki M, Morgan JI, McKinnon PJ. Requirement for Atm in ionizing radiation-induced cell death in the developing central nervous system. Science 1998;280:1089–91.

23. Gurley KE, Kemp CJ. Atm is not required for p53 induction and apoptosis in irradiated epithelial tissues. Mol Cancer Res 2007;5:1312–8.

24. Gorgoulis VG, Vassiliou LV, Karakaidos P, et al. Activation of the DNA damage checkpoint and genomic instability in human precancerous lesions. Nature 2005;434:907–13.

25. Bartkova J, Horejsi Z, Koed K, et al. DNA damage response as a candidate anti-cancer barrier in early human tumorigenesis. Nature 2005;434:864–70.

26. Bartkova J, Rezaei N, Liontos M, et al. Oncogene-induced senescence is part of the tumorigenesis barrier imposed by DNA damage checkpoints. Nature 2006;444:633–7.

27. Di MR, Fumagalli M, Cicalese A, et al. Oncogene-induced senescence is a DNA damage response triggered by DNA hyper-replication. Nature 2006;444:638–42.

28. Quintanilla M, Brown K, Ramsden M, Balmain A. Carcinogen-specific mutation and amplification of Ha-ras during mouse skin carcinogenesis. Nature 1986;322:78–80.

29. Burns PA, Kemp CJ, Gannon JV, et al. Loss of heterozygosity and mutational alterations of the p53 gene in skin tumors of interspecific hybrid mice. Oncogene 1991;6:2363–9.

30. Kemp CJ, Donehower LA, Bradley A, Balmain A. Reduction of p53 gene dosage does not increase initiation or promotion but enhances malignant progression of chemically induced skin tumors. Cell 1993;74:813–22.

31. Jonkers J, Meuwissen R, van der GH, et al. Synergistic tumor suppressor activity of BRCA2 and p53 in a conditional mouse model for breast cancer. Nat Genet 2001;29:418–25.

32. Kelly-Spratt KS, Gurley KE, Yasui Y, Kemp CJ. p19Arf suppresses growth, progression, and metastasis of Hras-driven carcinomas through p53-dependent and -independent pathways. PLoS Biol 2004;2:1138–49.

33. Rogakou EP, Pilch DR, Orr AH, Ivanova VS, Bonner WM. DNA double-stranded breaks induce histone H2AX phosphorylation on serine 139. J Biol Chem 1998;273:5858–68.

34. McManus KJ, Hendzel MJ. ATM-dependent DNA damage-independent mitotic phosphorylation of H2AX in normally growing mammalian cells. Mol Biol Cell 2005;16:5013–25.

35. Ichijima Y, Sakasai R, Okita N, et al. Phosphorylation of histone H2AX at M phase in human cells without DNA damage response. Biochem Biophys Res Commun 2005;336:807–12.

36. Koike M, Mashino M, Sugasawa J, Koike A. Dynamic change of histone H2AX phosphorylation independent of ATM and DNA-PK in mouse skin *in situ*. Biochem Biophys Res Commun 2007;363:1009–12.

37. Stiff T, O'Driscoll M, Rief N, et al. ATM and DNA-PK function redundantly to phosphorylate H2AX after exposure to ionizing radiation. Cancer Res 2004;64: 2390–6.

38. Palmero I, Pantoja C, Serrano M. p19ARF links the tumour suppressor p53 to Ras. Nature 1998;395:125–6.

39. Sherr CJ. Divorcing ARF and p53: an unsettled case. Nat Rev Cancer 2006; 6:663–73.

40. Harvey M, McArthur MJ, Montgomery CA, Jr., et al. Spontaneous and carcinogen-induced tumorigenesis in p53-deficient mice. Nat Genet 1993;5:225–9.

41. Jacks T, Remington L, Williams BO, et al. Tumor spectrum analysis in p53-mutant mice. Curr Biol 1994;4:1–7.

42. Purdie CA, Harrison DJ, Peter A, et al. Tumour incidence,spectrum and ploidy in mice with a large deletion in the p53 gene. Oncogene 1994;9:603–9.

43. Kemp CJ, Wheldon T, Balmain A. p53 deficient mice are extremely susceptible to radiation-induced tumorigenesis. Nat Genet 1994;8:66–9.

44. Matsuoka S, Ballif BA, Smogorzewska A, et al. ATM and ATR substrate analysis reveals extensive protein networks responsive to DNA damage. Science 2007;316:1160–6.

45. Christophorou MA, Ringshausen I, Finch AJ, Swigart LB, Evan GI. The pathological response to DNA damage does not contribute to p53-mediated tumour suppression. Nature 2006;443:214–7.

46. Liao MJ, Van Dyke T. Critical role for Atm in suppressing V(D)J recombination-driven thymic lymphoma. Genes Dev 1999;13:1246–50.

47. Bredemeyer AL, Sharma GG, Huang CY, et al. ATM stabilizes DNA double-strand-break complexes during V(D)J recombination. Nature 2006;442: 466–70.

48. Taylor AMR, Metcalfe JA, Thick J, Mak YF. Leukemia and lymphoma in ataxia telangiectasia. Blood 1996;87:423–38.

49. Vasioukhin V, Degenstein L, Wise B, Fuchs E. The magical touch: genome targeting in epidermal stem cells induced by tamoxifen application to mouse skin. Proc Natl Acad Sci U S A 1999;96:8551–6.

50. Donehower LA, Harvey M, Slagle BL, et al. Mice deficient for p53 are developmentally normal but susceptible to spontaneous tumours. Nature 1992; 356:215–21.

51. Timme TL, Thompson TC. Rapid allelotype analysis of p53 knockout mice. Biotechniques 1994;17:462–3.